Jurnal Penelitian Fisika dan Aplikasinya (JPFA)
Volume 14, Issue 01, June 2024
https://journal.unesa.ac.id/index.php/jpfa/
p-ISSN: 2087-9946
e-ISSN: 2477-1775

Laser-Induced Graphene Oxide on Polyimide Sheet: The Effect of Current Regulation on the Laser Power Stability

Lenny Intan Martila [1,2,a], Suryadi [2,b], Nursidik Yulianto [2,c], Yuliati Herbani [2,d], Isnaeni [2,e], Zainul Arifin Imam Supardi [1,f,*], Evi Suaebah [1,g], and Iyon Titok Sugiarto [2,h,*]

[1] Departement of Physics, Faculty of Mathematics and Science, State University of Surabaya
Ketintang, Surabaya, East Java 60231, Indonesia
[2] Research Center of Photonics, National Research and Innovation Agency
Building 442 Bj Habibie Science and Technological Park, South Tangerang, Banten 15314, Indonesia

e-mail: [a] lenny.20044@mhs.unesa.ac.id, [b] sury023@brin.go.id, [c] nursidik.yulianto@brin.go.id, [d] yuli018@brin.go.id, [e] isnaeni@brin.go.id, [f] zainularifin@unesa.ac.id, [g] evisuaebah@unesa.ac.id, and [h] iyon.titok.sugiarto@brin.go.id
* Corresponding Author

Received: 5 March 2024; Revised: 19 May 2024; Accepted: 12 June 2024

Abstract

Graphene oxide is a two-dimensional substance that shares the same structure as graphene and can be produced using several methods. The difficulty for green technology lies in developing a cost-effective and efficient method to produce graphene and graphene oxide without relying on chemical processes. A highly sustainable technology involves the use of a laser diode, which is both cost-effective and environmentally friendly. This technique produces a material known as laser-induced graphene/graphene oxide (LIG/LIGO). From a commercial standpoint, the laser diode is typically purchased without an electronic stabilizer component. Nevertheless, laser stability is crucial for the production process of LIG/LIGO. The objective of our study is to examine the impact of laser current management on the production of graphene on a polyimide (PI) sheet utilizing a 450 nm diode laser. The laser controller we utilize is the National Instruments (NI) PXIe-1085 device. The optical power of the laser diode was measured between 0.21 and 0.79 W. After the laser current was stabilized, the power slightly shifted, ranging from 0.18 to 0.86 W. Both experiments were conducted with a current range of 0.3 to 1 A. Before regulation, the laser diode experiences current fluctuations in the range of around 0.01 to 0.03 A. The study findings highlight the significance of laser current management in manufacturing LIG/LIGO by ensuring a consistent and precise laser power output, hence minimizing flaws in the final product. However, the analysis reveals that graphene oxide is the predominant yield in this characterization. This fact is caused by the presence of a graphene layer not exposed to the surface during measurement. This approach provides several benefits, such as the capacity to produce graphene/GO in a targeted, non-chemical, and fast manner, as well as its potential for diverse applications.

Keywords: *laser diode; stability; fluctuation; polyimide; laser-induced graphene oxide*

How to cite: Martila LI, Suryadi, Yulianto N, Herbani Y, Isnaeni, Supardi ZAI, Suaebah E, and Sugiarto T. Laser-Induced Graphene Oxide on Polyimide Sheet: The Effect of Current Regulation on the Laser Power Stability. *Jurnal Penelitian Fisika dan Aplikasinya (JPFA)*. 2024; 14(1): 99-111. DOI: https://doi.org/10.26740/jpfa.v14n1.p100-112.

© 2024 Jurnal Penelitian Fisika dan Aplikasinya (JPFA). This work is licensed under CC BY-NC 4.0

DOI: 10.26740/jpfa.v14n1.p100-112

INTRODUCTION

Currently, lasers significantly impact various aspects of contemporary society, including medical, manufacturing, and electronics. Lasers play a crucial part in the manufacturing process of graphene, a carbon allotrope consisting of a single layer of carbon atoms arranged in a hexagonal shape [1]. Graphene has versatile applications in various industries, including energy, materials, and electronics, where it serves as a fundamental material for producing flexible sensors. Creating graphene using lasers is called laser-induced graphene (LIG) technology, which is simple and time-efficient. Nevertheless, forming LIG often requires substantial laser power until the LIG structure experiences structural harm [2]. Diode lasers, which are a type of semiconductor lasers, are applicable in the LIG process. Laser diodes are commonly utilized in many application domains [3,4] due to their availability in multiple wavelengths, ease of procurement, cost-effectiveness, and relatively high-power output [5,6]. Laser diodes, despite their benefits, have a few drawbacks. These include an elliptical beam shape and sensitivity to ambient conditions that might impact the wavelength [7].

The issue of laser power instability remains a concern for diode lasers. The laser power is often derived from the conversion of current into laser power. However, the instability is primarily caused by external noise or changes in the current outside the laser. Various environmental conditions can influence the laser beam, leading to changes in its current. Instances such as the descent of dust particles into the path of the beam or the oscillation of mechanical components, alterations in temperature, and airflow can lead to oscillations that cause changes in the properties of the beam [8]. This problem could impede the use of a laser diode in various applications, including laser-induced graphene, laser writing, magnetometers, atomic clocks, spectroscopy, laser frequency standards, interferometry, and gravitational wave detection. These applications rely on a laser output that is consistent and stable [9–11]. The study conducted by Velasco et al. on the performance of LIG micro-supercapacitors demonstrates that laser power is the primary factor in the formation of LIG in thin layers. The laser power has an impact on both the laser fluence and the scanning speed [12]. A separate investigation conducted by Kulyk et al. demonstrated that the manipulation of laser power settings, laser scanning speed, and distance between the laser and the paper surface had a notable impact on the formation of LIG on paper substrates [2]. These two research experiments have conclusively demonstrated the efficacy of the LIG technique in producing graphene, thanks to the utilization of a highly stable CO_2 laser. While some reports are available for LIG production using laser diodes, none of them discuss the stability of the laser used in their experiments [13–17]. The laser power instability may specifically cause a decrease in the resistance value, carbon atom percentage, and porosity level of the created LIG. Thus, laser stability has a crucial impact on controlling the properties of the resulting LIG [18].

In this work, we investigate the creation of LIG from a polyimide sheet using a low-cost 450nm diode laser. The focus of the study is on the stability of laser intensity during the formation process. Although LIG can typically be produced effortlessly using a high-powered CO_2 laser, this study seeks to examine the feasibility of creating graphene using a 450nm diode laser with a regulated current. The reason for this is that graphene and polyimide have a strong tendency to absorb light in the near ultraviolet (UV) range. Therefore, using a laser with a wavelength between 405 nm and 450 nm and an output power ranging from 15 to 1000 mW can effectively generate carbonization in the feedstock [15]. This study has the potential to provide a new method for producing LIG using a low-cost diode laser that is readily available in the market.

METHOD

This study will undertake three stages of the measurement process. The first step involves assessing the relationship between the injection current of the 450 nm laser diode (GSR-B009) and the resulting optical power output of the laser. This characterization is done both before and after regulating the injection laser current. The laser diode has a maximum electrical current of 1.0 A. Using a power meter (Newport Model 843-R), the laser current was characterized by measuring the fluctuations in laser diode current from 0.3 to 1.0 A. This measurement was conducted for a duration of 30 seconds to monitor and ensure the stability of the laser output. The second step involves assessing the beam spot of the laser diode under both controlled and uncontrolled laser current settings. The fluctuation of the power laser during the procedure must be minimized. To ensure that the 450 nm laser diode is driven with consistent laser power, dependable current sources are necessary. A Source Measurement Module (SMU) from National Instrument is employed for this purpose (Figure 1 (a)). The PXIe-1085 PXI express chassis is the host of the SMU module PXI-4130, which can supply a stable and programmable current of up to 2A [19]. This second step involved exposing a 0.15mm thick polyimide sheet (PI) to the diode laser beam for a duration of 1 second while varying the laser current from 0.3 A to 1.0 A to form a LIG crater. The crater diameter was measured as a laser beam spot using a 1200X Microscope Digital Portable 7" LCD Video Microscope 12MP (Huiley). The final step is to write the PI sheet directly using a laser to produce a large area of LIG, as depicted in Figure 1 (a)-(b). The laser beam was focused using a 10 cm focusing lens and directed perpendicular to the PI sheet, which had a size pattern of 5x5 mm, as shown in Figure 1 (b). A constant scanning speed of the micro-stage at 5 mm/s was used. The pitch distance (a) was established at 0.3 mm due to the absence of vacant space between the beam spots in the formed pattern at this distance, which leads to a more consistent LIG structure. The x-y micro stage was developed to regulate the laser movement to achieve a uniform surface with micrometer precision in the X and Y axes [20]. This resulting pattern, which was previously designed, is illustrated in Figure 1 (c). The resulting LIGs were further examined using FESEM (JEOL JIB-4700F) and a Raman spectrometer (HORIBA HR550 modular) for morphological and material phase analysis.

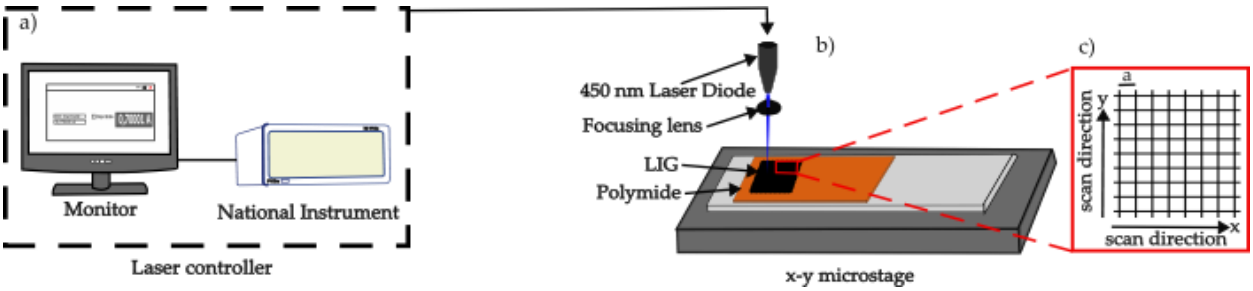

Figure 1. Experimental Setup of LIG Process on Polyimide Sheet: (a) Laser Controller System, (b) LIG Engraving on the PI Sheet, and (c) Pattern Design of LIG on PI Sheet

RESULTS AND DISCUSSION

Characterization of 450 nm Laser Diode Current Toward the Output Power

In order to generate LIG, it is imperative to maintain electrical current stability, as this parameter is associated with the laser diode's optical output power. Thus, the regulation of the electric current is a critical component in the attainment of laser stability. Figure 2 illustrates the optical power characteristics that are contingent upon electrical current. The blue curve in Figure 2 indicates that the optical power laser was unstable, with a maximal optical power of less than 0.8 W at 1 A. Optical power was measured using a laser power meter after the electrical current input was varied from 0.3 A to 1.0 A, and the stability test was conducted. Following the implementation of an additional stabilization system, the optical power was significantly stabilized, as evidenced by the linearity graph and the control value of 0.9 Watt/Ampere, as illustrated by the red curve in Figure 2. The laser power value is 0.18 W at a current of 0.3 A and 0.86 W at a current of 1.0 A, as indicated in this figure. Compared to the blue curve, the power value before being controlled is greater than after at a laser diode current of 0.3 A.

Conversely, the laser diode power value is higher after being controlled at a laser diode current of 0.4 A to 1.0 A. This is because the laser diode current fluctuations can be effectively suppressed to a minimum level after being controlled, which leads to a laser power output that is significantly more consistent and stable. The laser's optimal performance can be achieved through the control of the laser diode current. It is also evident from this characterization that the results of laser current characterization in relation to laser power are consistent with the theory that the laser power value increases as the laser current increases. This implies that the laser current is directly proportional to the laser intensity.

As control feedback, the SMU module has the capability to both set and receive the value of electrical current. The reading electrical current that induces fluctuations in the optical power laser precedes the stabilization. Typically, the laser current fluctuates between 0.01 and 0.02 A [21]. In most applications, the signal-to-noise ratio can be reduced by the high frequency of the laser output. For instance, before being regulated at 0.3 A, the laser current value fluctuated to 0.02 A. In addition, the laser current value of 1.0 A prior to control corresponds to the same laser current fluctuation of 0.02 A, which is classified as system noise. Consequently, the signal-to-noise ratio calculation will consider the ratio of the laser's light output power to the magnitude of laser current fluctuations that result in an unstable laser power.

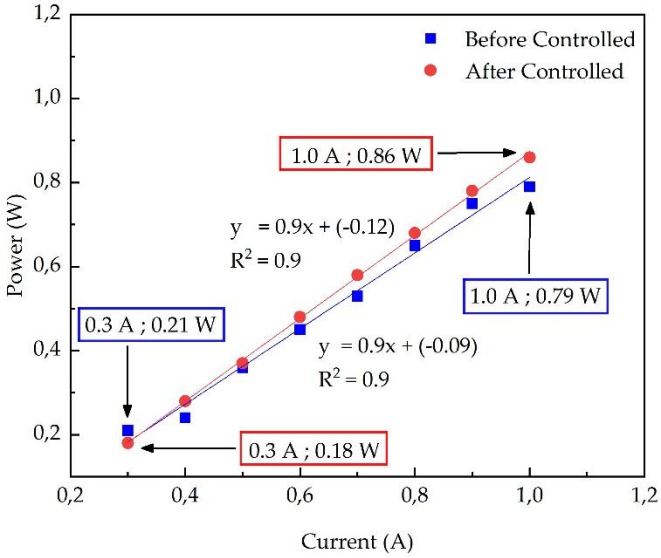

Figure 2. Laser Current Stability in Terms of Laser Output Power as A Function of The Input Current, Before (Red Circle) and After (Blue Square) Controlled

Upon the implementation of the laser controller, the laser diode 450 nm maintained a consistent current value, as evidenced by the consistent beam point size. Unlike the circumstances prior to the regulation of laser diode current, the diameter of the beam point increases as the laser diode current increases. Additionally, the laser current will also fluctuate during the scanning process, influencing the pattern generated during the LIG manufacturing process if it is not regulated. A black crater is acquired from the laser diode shot directly at the polyimide, as illustrated in Figure 3. The crater dimension was examined using a digital microscope to ascertain its diameter, which can be considered as the laser beam spot. Figures 3 (a) and (b) illustrate the results of the spot diameter measurement prior to and subsequent to laser current control.

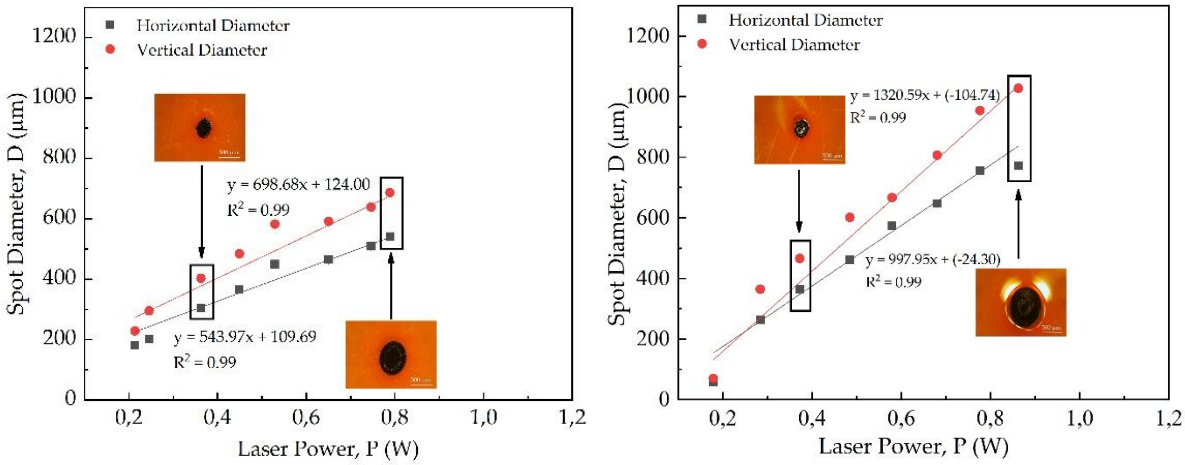

(a) (b)

Figure 3. The Beam Crater Diameter Versus Laser Power: a) Before and b) After Laser Current-Controlled

According to Figure 3, the correlation graph between the beam spot laser diameter and the laser diode power, the two variables are directly proportional or linear. It can be observed that the diameter of the beam point expands with the increase in power of the laser diode. Beam point laser diameter size is directly proportional to laser power in both scenarios. Figure 3 (a) illustrates the impact of laser power on the beam point diameter before regulating laser current. The presence of uncontrolled fluctuations in the laser diode current influences the degree of variation in the beam spot's diameter. The data distribution in Figure 3 (b) is more condensed and concentrated around the trend line, indicating a linear relationship between the laser diode power and the beam spot diameter of the laser diode that was irradiated onto the PI sheet. The comparison of the two graphs demonstrates that the controlled laser produces a superior beam point compared to the uncontrolled laser. In addition, this underscores the significance of regulating the laser current in laser experiments or applications in our research to produce LIG. Despite the fact that laser diodes are relatively efficient, low-cost, and do not require high-voltage operation, they exhibit poor stability [22].

The PI sheet undergoes a transformation from orange to black as the pattern design conforms to laser irradiation, as evidenced by the results of this experiment. The rectangular line used for pattern scanning is 0.5 × 0.5 cm. Using this pattern, it requires 1 minute and 52 seconds to produce a single sample. This experiment was conducted by altering the laser current from 0.4 to 1.0 A, which is equivalent to an optical laser power of 0.28 to 0.86 W. Based on the photographic evidence, the polyimide surface did not exhibit any color change at a laser power of 0.18 W (refer to Figure 4 (a)). However, alterations began to appear at a laser power of 0.28 W (refer to Figure 4 (b)). Consequently, experiments were conducted at a laser intensity of 0.28 – 0.86 W, at which point the PI surface begins to be damaged at 0.66 W (Figure 4 (f)). The optical photograph of the PI sheet after irradiation by a 450 nm laser diode within a 0.5 × 0.5 cm pattern with a laser power range of 0.28 – 0.86 W, following laser diode current control, is depicted in Figure 4 (a)-(h).

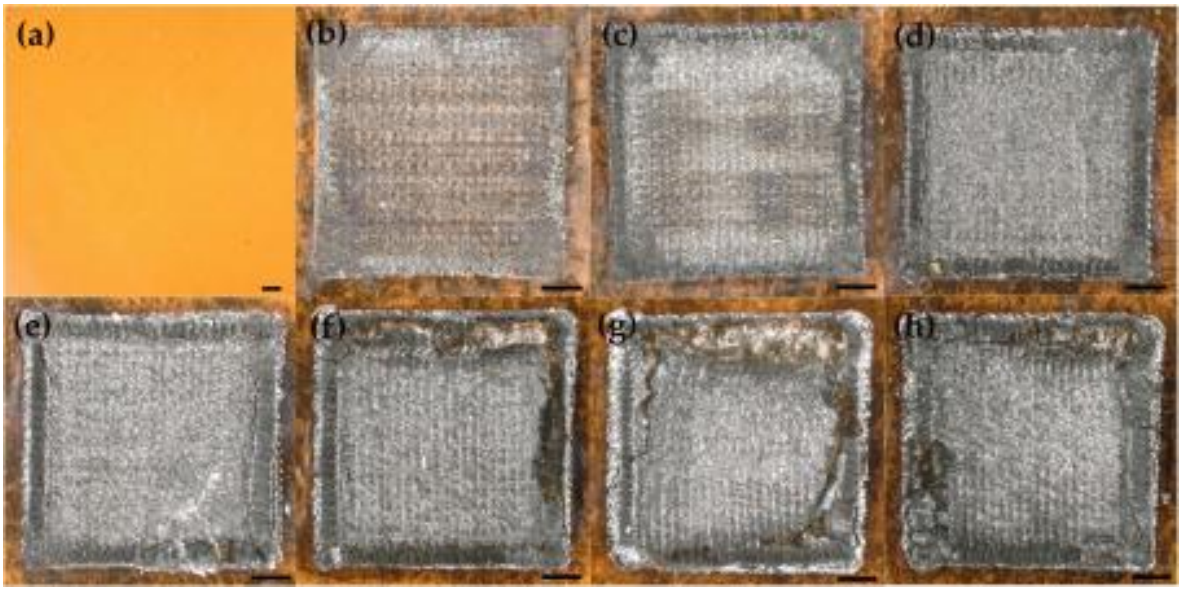

Figure 4. Optical Photograph of the (a) PI with 20× Magnification(b) LIG Pattern on the PI Sheet Under Different Laser Powers After Laser Current Control at Laser Power 0.28 W (c) 0.37 W (d) 0.48 W (e) 0.58 W (f) 0.66 W (g) 0.78 W (h) 0.86 W with 30× Magnification. Scale Bar: 500µm

According to Figure 4, the likelihood of graphene forming on the polyimide sheet falls between the power levels of 0.37 W and 0.86 W. The incomplete combustion of the polyimide at a laser power of 0.28 W is evident from the orange color observed in the resulting pattern (Figure 4 (b)). The laser power of 0.28 W is insufficient to adequately convert polyimide into graphene due to its poor energy output. When a laser is directed at a polymer surface, it absorbs energy from the polymer, leading to its breakdown at the specific location where it is irradiated. Increasing the laser power leads to a faster combustion process on the PI sheet [7]. Figure 4 (f)-(h) reveals the presence of cracks in the LIG structure generated with laser power ranging from 0.66 to 0.86 W. This demonstrates that excessive laser power leads to the inability to generate LIG. Moreover, the lack of stability in the laser might also impact the composition of the resulting LIG.

The fluctuation of the laser current in the LIG fabrication technique might lead to undesired fluctuations in the heating or scanning process of the PI sheet. It can result in unmanageable alterations in the structure and quality of the graphene generated. The attributes and qualities of LIG exhibit variability and present challenges in terms of precise measurement and accurate prediction. Consequently, the quality control of LIG production becomes more challenging and can potentially impact the performance or application of the LIG. Hence, it is crucial to uphold the stability of the laser current to guarantee the excellence and uniformity of the LIG output.

Raman Characterization

The Raman spectroscopy graph displays a Raman shift, representing the alteration in the wavelength of photons scattered by molecules within the sample [23]. The highest point of the spectrum on the Raman graph can be associated with the frequency vibration of the molecule, their precursor, or the terminal part of the molecule [24]. A more detailed analysis of the carbonaceous surface LIG on a polyimide sheet was carried out using Raman spectroscopy (HORIBA HR550) with an excitation wavelength of 532 nm. Figure 5 displays normal Raman spectra of the PI sheet and the resulting LIG at various laser powers.

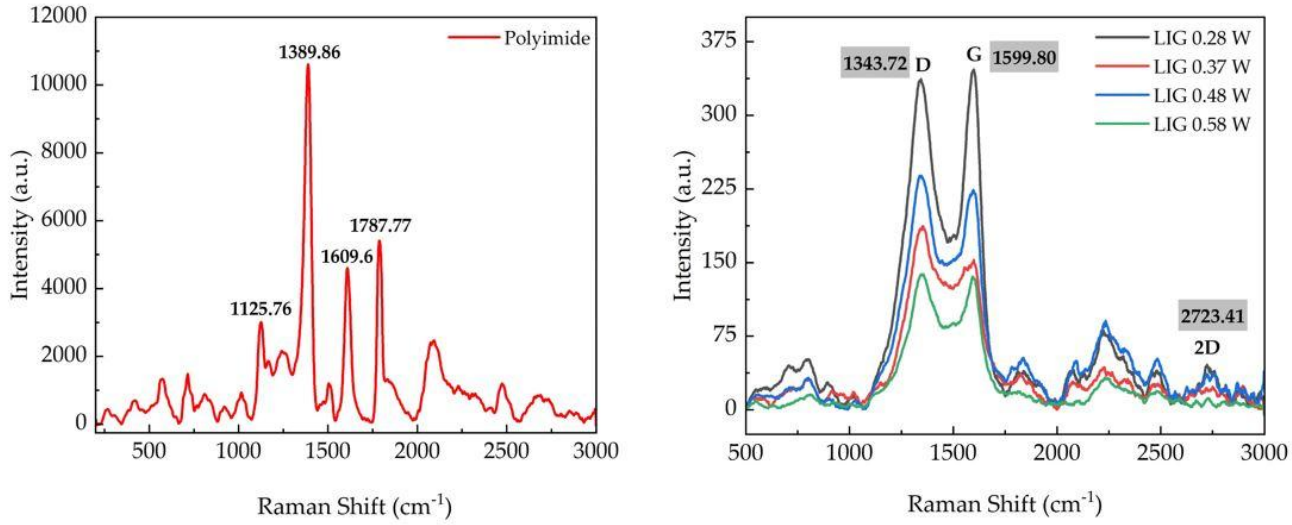

(a) (b)

Figure 5. Raman Spectra of (a) Polyimide Sheet and (b) LIG

According to Figure 5 (a), the Raman spectroscopy graph of raw PI exhibits four distinct peaks at the following wavenumbers: 1125.76, 1389.86, 1609.6, and 1787.77 cm^{-1}. A C-N-C chemical bond was established with transverse vibrations as its vibrational properties at a wavelength of 1125.76 cm^{-1}. Similarly, the spectrum at a frequency of 1389.86 cm^{-1} likewise exhibited C-N-C bonds and displayed axial vibrations' vibrational properties. In the 1609.6 cm^{-1} spectrum, vibrational characteristics are related to carboxylic acid ring vibrations. A C = O bond was created at a frequency of 1787.77 cm^{-1}, with stretching as its vibrational characteristic.

The Raman spectra of LIG or graphitized materials exhibit a distinct feature: the occurrence of symmetrical 2D peaks [2]. Figure 5 (b) displays the graph representing the D, G, and 2D peaks. The D peak signifies a defect or a bent sp^2-carbon bond [25]. Peak G corresponds to the peak resulting from the vibrations of carbon-carbon bonds in the sp^2-lattice [26]. It is the primary Raman band observed in all carbons that are sp^2 hybridized [25]. By contrast, the 2D peak is caused by phonon vibrations in the second-order region [25]. The presence of many 2D peaks suggests the development of carbon with a graphitized structure, while the single peak in the Lorentzian spectrum shows the process of graphene formation [14]. The presence of 2D peaks is commonly employed as an indication of the accumulation of carbon atom layers in the graphene structure [7]. Graphene was created using laser irradiation, generating extremely high temperatures in the targeted region. This leads to the cleavage of C-O, C=O, and N-C bonds, resulting in carbon atoms' reorganization and a graphene structure [27]. Concurrently, the left carbon atoms will recombine and be emitted as gas.

Figure 5 (b) displays Raman spectra of LIG obtained with various laser power. This figure shows that the LIG Raman spectra exhibit three distinct peaks: D, G, and 2D. The intensity and shape of the D, G, and 2D peaks in the Raman spectra of LIG indicate the presence of damaged layers. The D peak in graphite and high-quality graphene is frequently characterized by its comparatively low intensity [28]. When the intensity of the D peak is high, it indicates a significant presence of damage or flaws in the material. The strength of the D peak can determine the level of defects. Figure 5 (b) indicates that the D, G, and 2D peaks were located at a wavenumber of 1343.72, 1599.80, and 2723.41 cm^{-1}, respectively. The G peak differs from the D peak, indicating the number of graphene layers. Therefore, the G peak is very sensitive to the existing layers, so the G peak can be used as a reference for determining the thickness of the layer. The number of layers can be known by using equation (1):

$$\omega_G = 1581.6 + \frac{11}{1+n^{1.6}} \quad (1)$$

where ω_G is the position of the G peak in wave numbers, and n is the number of layers [28]. Based on the equation, the value of n is 0.56, so the LIG obtained is multi-layered in this work. In addition, there was also the 2D peak present in the spectra, and it can be used to determine the thickness of the graphene layer [28]. The 2D peak has a much smaller intensity than the D and G peaks, indicating that graphene has not yet been formed in this case. Thus, this experiment obtained laser-induced graphene oxide (LIGO), which is indicated by the low intensity of the 2D peak and the low I_{2D}/I_G value. The I_{2D}/I_G values obtained at laser power of 0.28, 0.37, 0.48, and 0.58 W were 0.116, 0.181, 0.163, and 0.139, respectively. A higher I_{2D}/I_G ratio indicates an improved quality of graphene [11]. From here on, we stated LIGO rather than LIG for the structure generated on the PI sheet.

FE-SEM Characterization

Figure 6 shows optical and FE-SEM images of LIGO fabricated after controlling the laser current. Figure 6 (a) shows a top-viewed optical image of a large area of LIG fabricated at a laser power of 0.58 W, and Figure 6 (b) is the corresponding FE-SEM image of the magnified area. In Figure 6 (b), the LIGO's surface morphology exhibits homogeneity with grooves created by linear laser scanning. The figure also reveals that the LIGO structure is relatively intact with few visible cracks. The lack of cracks indicates that the cracking is likely to be at a low level. This can be seen as a positive aspect, as the indication of a few cracks can be connected to the higher quality of the graphene. The presence of a few cracks can also be interpreted as a sign that the layer structure on the LIGO surface can support good mechanical stability.

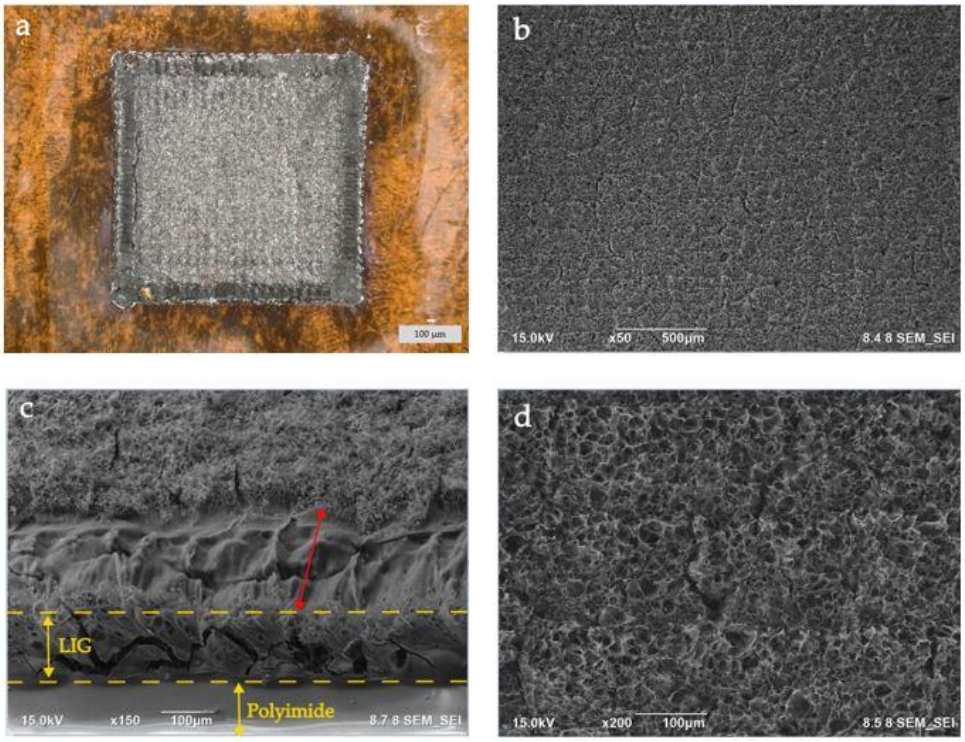

Figure 6. (a) Optical Photograph, and (b-d) FESEM Images of LIGO After Controlling the Laser Current. (b) Top-Viewed Area, (c) Edge Area (30° titled) and (d) Top Viewed Area at Higher Magnification of LIGO Surface

Figure 6(c) is the tilted FESEM image of the LIG edge, the area where the laser scans twice. From this figure, we can predict the thickness of the LIGO, which is ~155 μm, as shown by the distance between yellow dashed lines. The area indicated by the red line in Figure 6 (c) was seen to be a rough, nonporous surface with high oxidation. This may result from two repetitions of LIGO pattern formation by the laser diode on the polyimide [29]. As shown in Figure 6 (d), LIGO has a foam-like porous structure, where the presence of porous is generated by gas that appears due to heteroatom recombination [30]. The porous structure of the LIGO provides significant benefits in electrochemical performance, as it can accelerate the diffusion of electrolytes into the electrode through an increase in accessible surface area [31]. LIGO has an irregular structure with empty spaces, showing various electrical properties [32]. LIGO produced from Polyimide sheets easily

forms porous structures due to the properties of polyimide, which contain a charge-transfer complex [33]. The many irregular pores in the microstructures indicate that graphene was not formed in this experiment, but graphene oxide was formed, called laser-induced graphene oxide (LIGO).

This study demonstrates the significance of laser current regulation in maintaining laser stability across different applications, focusing on laser-induced graphene. Nevertheless, it is crucial to acknowledge the significant constraints associated with this study. While it has been demonstrated that regulating the current of the laser diode yields superior outcomes in the irradiation procedure, the investigation reveals that the approach generates graphene oxide instead of the anticipated graphene. This emphasizes the significance of comprehensively grasping the characteristics and mechanisms associated with LIG development in order to avoid unfavorable outcomes. This work also highlights the need for additional research to enhance the efficiency of the LIG creation process using a laser diode. By gaining a deeper understanding of the elements that impact the conversion of graphene to graphene oxide, future studies can enhance the present regulation of the laser diode to generate more refined and superior-quality graphene, which can be effectively employed for technological advancements in many applications.

CONCLUSION

This study examined the impact of stabilizing the current of a 450 nm laser diode on the production of laser-induced graphene (LIG) and laser-induced graphene oxide (LIGO). The experimental results demonstrate that the manipulation of laser current plays a crucial role in the production of LIG later on. In the absence of current regulation of the laser diode, the outcome is a defective and inconsistent LIG structure. Thus, it can be inferred that optimal performance of the laser diode in manufacturing LIG is achieved through precise control of the laser current. Nevertheless, the outcome of this study did not provide the anticipated graphene but rather graphene oxide, specifically referred to as laser-induced graphene oxide (LIGO). This study serves as a fundamental foundation for future investigations in advancing the development of more refined and regulated processes for forming LIG to enhance the purity and excellence of the resulting graphene. Further investigation has the potential to yield substantial breakthroughs in the utilization of graphene and graphene oxide across various domains of technology and science. This approach provides several benefits, such as the capability to produce graphene in a targeted, non-chemical, and fast manner and its potential for diverse applications.

ACKNOWLEDGMENT

This work was done with full support from the Research Center for Photonics, National Research and Innovation Agency - BRIN. The authors acknowledged Mrs. Zahra S. Mujahidah as a technician in the Advanced Physical Characterization Laboratory, Division of Research and Innovation Infrastructure BRIN for Raman spectroscopy measurement.

AUTHOR CONTRIBUTIONS

The manuscript was written with contributions from all authors. All authors have approved the final version of the manuscript. L. I. Martila and I. T. Sugiarto performed laser micromachining measurements, fabricated the LIG, and wrote the original Draft; Suryadi performed the electronic instrumentation; N. Yulianto, I.T. Sugiarto, and Y. Herbani performed FE-SEM and Raman characterization; N.Yulianto, I. T. Sugiarto, Y. Herbani, and Isnaeni revised the paper, managed the

project, and supervised the work; Z. A. I. Supardi as a supervisor responsible for academic and experimental content; E. Suaebah as an academic content examiner.

DECLARATION OF COMPETING INTEREST

The authors declare that they have no known competing financial interests or personal relationships that could have appeared to influence the work reported in this paper.

REFERENCES

[1] Murthy HCA, Ghotekar S, Vinay Kumar B, and Roy A. Graphene: A Multifunctional Nanomaterial with Versatile Applications. *Advances in Materials Science and Engineering*. 2021; **2021**(1): 2418149. DOI: https://doi.org/10.1155/2021/2418149.

[2] Kulyk B, Silva BFR, Carvalho AF, Silvestre S, Fernandes AJS, Martins R, et al. Laser-Induced Graphene from Paper for Mechanical Sensing. *ACS Applied Materials and Interfaces*. 2021; **13**(8): 10210-10221. DOI: https://doi.org/10.1021/acsami.0c20270.

[3] Winingsih PH. Rancang Bangun Laser Untuk Pembelajaran Optika Dalam Menentukan Indeks Bias Dan Difraksi Kisi. *Science Tech: Jurnal Ilmu Pengetahuan Dan Teknologi*. 2015; **1**(1): 77–82. DOI: https://doi.org/10.30738/jst.v1i1.482.

[4] Yan Y, Zheng Y, Sun H, and Duan J. Review of Issues and Solutions in High-Power Semiconductor Laser Packaging Technology. *Frontiers in Physics*. 2021; 9: 1–16. DOI: https://doi.org/10.3389/fphy.2021.669591.

[5] Hasanah N. Analisis Penggunaan Cahaya Laser Untuk Menentukan Indeks Bias Kaca. *Jurnal Sains dan Teknologi*. 2022; **12**(1): 28–33.

[6] Michalik M, Szymańczyk J, Stajnke M, Ochrymiuk T, and Cenian A. Medical Applications of Diode Lasers: Pulsed Versus Continuous Wave (cw) Regime. *Micromachines*. 2021; **12**(6): 1-15. DOI: https://doi.org/10.3390/mi12060710.

[7] Sholahuddin. *Studi Pembuatan Laser Induced Graphene pada Lembaran Polyimide dengan Laser Dioda 450 nm*. Undergraduate Thesis. Unpublished. Jakarta: UIN Syarif Hidayatullah Jakarta; 2023.

[8] Seifert F. *Power Stabilization of High Power Lasers for Second Generation Gravitational Wave Detectors*. PhD Thesis. Unpublished. Germany: Leibniz University Hannover; 2010.

[9] Yu H, Gai M, Liu L, Chen F, Bian J, and Huang Y. Laser-Induced Direct Graphene Patterning: from Formation Mechanism to Flexible Applications. *Soft Science*. 2023; **3**(4): 1–33. DOI: https://doi.org/10.20517/ss.2022.26.

[10] Jeong SY, Ma YW, Lee JU, Je GJ, and Shin BS. Flexible and Highly Sensitive Strain Sensor Based on Laser-Induced Graphene Pattern Fabricated by 355 nm Pulsed Laser. *Sensors*. 2019; **19**(22): 4867. DOI: https://doi.org/10.3390/s19224867.

[11] Sartanavicius A, Zemgulyte J, Ragulis P, Ratautas K, and Trusovas R. Laser-Induced Graphene in Polyimide for Antenna Applications. *Crystals*. 2023; **13**(7): 1003. DOI: https://doi.org/10.3390/cryst13071003.

[12] Velasco A, Ryu YK, Hamada A, de Andrés A, Calle F, and Martinez J. Laser-Induced Graphene Microsupercapacitors: Structure, Quality, and Performance. *Nanomaterials*. 2023; **13**(5): 788. DOI: https://doi.org/10.3390/nano13050788.

[13] Romero FJ, et al. In-depth Study of Laser Diode Ablation of Kapton Polyimide for Flexible Conductive Substrates. *Nanomaterials*. 2018; **8**(7): 517. DOI:

https://doi.org/10.3390/nano8070517.

[14] Stanford MG, Zhang C, Fowlkes JD, Hoffman A, Ivanov IN, Rack PD, et al. High-Resolution Laser-Induced Graphene: Flexible Electronics Beyond the Visible Limit. *ACS Applied Materials and Interfaces*. 2020; **12**(9): 10902–10907. DOI: https://doi.org/10.1021/acsami.0c01377.

[15] Li G. Direct Laser Writing of Graphene Electrodes. *Journal of Applied Physics*. 2020; **127**(1): 010901. DOI: https://doi.org/10.1063/1.5120056.

[16] Kothuru A and Goel S. Leveraging 3-D Printer with 2.8-W Blue Laser Diode to Form Laser-Induced Graphene for Microfluidic Fuel Cell and Electrochemical Sensor. *IEEE Transactions on Electron Devices*. 2022; 69(3): 1333–1340. DOI: https://doi.org/10.1109/TED.2022.3140707.

[17] Avinash K and Patolsky F. Laser-Induced Graphene Structures: From Synthesis and Applications to Future Prospects. *Materials Today.* 2023; **70**: 104–136. DOI: https://doi.org/10.1016/j.mattod.2023.10.009.

[18] Cheng L, Guo W, Cao X, Dou Y, Huang L, Song Y, et al. Laser-Induced Graphene for Environmental Applications: Progress and Opportunities. *Materials Chemistry Frontiers*. 2021; **5**(13): 4874–4891. DOI: https://doi.org/10.1039/D1QM00437A.

[19] National Instruments Corp. *Cascading the Outputs of the NI PXI-4130 Source Measure Units*. Available from: https://www.ni.com/en/support/documentation/supplemental/12/cascading-the-outputs-of-the-ni-pxi-4130-source-measure-units.html [accessed 8 January 2024]

[20] Ren M, Zhang J, and Tour JM. Laser-Induced Graphene Synthesis of Co3O4 in Graphene for Oxygen Electrocatalysis and Metal-air Batteries. *Carbon*. 2018; **139**: 880–887. DOI: https://doi.org/10.1016/j.carbon.2018.07.051.

[21] Tricot F, Phung DH, Lours M, Guérandel S, and De Clercq E. Power Stabilization of A Diode Laser with an Acousto-optic Modulator. *Review of Scientific Instruments*. 2018; **89**(11): 113112. DOI: https://doi.org/10.1063/1.5046852.

[22] Abedin KM, Al Jabri AR, and Mujibur Rahman SM. Power Stability of Different Lasers and its Effect on the Outcome of Phase-stepping Shearography Experiments. *Results in Optics*. 2023; **12**: 100490. DOI: https://doi.org/10.1016/j.rio.2023.100490.

[23] Adya A K and Canetta E. Nanotechnology and Its Applications to Animal Biotechnology. In Ashish S. Verma, Anchal Singh, *Animal Biotechnology*. Massachusetts: Academic Press; 2014: 247–263. DOI: https://doi.org/10.1016/B978-0-12-416002-6.00014-6.

[24] Yoon H, Kim BH, Kwon SH, Kim DW, and Yoon YJ. Polyimide Photodevice without A Substrate by Electron-beam Irradiation. *Applied Surface Science.* 2021; **570**: 151–185. DOI: https://doi.org/10.1016/j.apsusc.2021.151185.

[25] Mahmood F, Zhang C, Xie Y, Stalla D, Lin J, and Wan C. Transforming Lignin Into Porous Graphene Via Direct Laser Writing for Solid-State Supercapacitors. *RSC Advances*. 2019; **9**(39): 22713–22720. DOI: https://doi.org/10.1039/c9ra04073k.

[26] Martins L, Kulyk B, Theodosiou A, Ioannou A, Moreirinha C, Kalli K, et al. Laser-Induced Graphene from Commercial Polyimide Coated Optical Fibers for Sensor Development. *Optic and Laser Technology*. 2023; **160**: 109047. DOI: https://doi.org/10.1016/j.optlastec.2022.109047.

[27] Guo Y, Zhang C, Chen Y, and Nie Z. Research Progress on the Preparation and Application of Laser-Induced Graphene Technology. *Nanomaterials*. 2022; 12(2): 23–36. DOI: https://doi.org/10.3390/nano12142336.

[28] Wall M. *The Raman Spectroscopy of Graphene and the Determination of Layer Thickness*. Madison: Thermo Scientific; 2022. Available from:

https://tools.thermofisher.com/content/sfs/brochures/AN52252_E+1111+LayerThkns_H_1.pdf.

[29] Li Y, Luong DX, Zhang J, Tarkunde YR, Kittrell C, Sargunaraj F, et al. Laser-Induced Graphene in Controlled Atmospheres: From Superhydrophilic to Superhydrophobic Surfaces. *Advanced Materials*. 2017; **29**(27): 1700496. DOI: https://doi.org/10.1002/adma.201700496.

[30] Liu M, Wu JN, and Cheng HY. Effects of Laser Processing Parameters On Properties Of Laser-Induced Graphene by Irradiating CO2 Laser On Polyimide. *Science China Technological Sciences*. 2022; **65**(1): 41–52. DOI: https://doi.org/10.1007/s11431-021-1918-8.

[31] Mahmood F, Mahmood F, Zhang H, Lin J, and Wan C. Laser-Induced Graphene Derived from Kraft Lignin for Flexible Supercapacitors. *ACS Omega*. 2020; **5**(24): 14611–14618. DOI: https://doi.org/10.1021/acsomega.0c01293.

[32] An JW, Hyeong SK, Kim KM, Lee HR, Park J won, Kim TW, et al. Facile Synthesis of Laser-Induced Graphene Oxide and its Humidity Sensing Properties. *Carbon Letters*. 2024; **34**: 1173–1185. DOI: https://doi.org/10.1007/s42823-023-00672-3.

[33] Hong S, Kim J, Jung S, Lee J, and Shin BS. Surface Morphological Growth Characteristics of Laser-Induced Graphene with UV Pulsed Laser and Sensor Applications. *ACS Materials Letters*. 2023; **5**(4): 1261–1270. DOI: https://doi.org/10.1021/acsmaterialslett.2c01222.